A spatial ecosystem and populations dynamics model (SEAPODYM) – Modeling of tuna and tuna-like populations

Patrick Lehodey [a,*], Inna Senina [a], Raghu Murtugudde [b]

[a] MEMMS (Marine Ecosystems Modelling and Monitoring by Satellites), CLS, Satellite Oceanography Division, 8-10 rue Hermes, 31520 Ramonville, France
[b] ESSIC, Earth Science System Interdisciplinary Center, University of Maryland, USA

ARTICLE INFO

ABSTRACT

An enhanced version of the spatial ecosystem and population dynamics model SEAPODYM is presented to describe spatial dynamics of tuna and tuna-like species in the Pacific Ocean at monthly resolution over 1° grid-boxes. The simulations are driven by a bio-physical environment predicted from a coupled ocean physical–biogeochemical model. This new version of SEAPODYM includes expanded definitions of habitat indices, movements, and natural mortality based on empirical evidences. A thermal habitat of tuna species is derived from an individual heat budget model. The feeding habitat is computed according to the accessibility of tuna predator cohorts to different vertically migrating and non-migrating micronekton (mid-trophic) functional groups. The spawning habitat is based on temperature and the coincidence of spawning fish with presence or absence of predators and food for larvae. The successful larval recruitment is linked to spawning stock biomass. Larvae drift with currents, while immature and adult tuna can move of their own volition, in addition to being advected by currents. A food requirement index is computed to adjust locally the natural mortality of cohorts based on food demand and accessibility to available forage components. Together these mechanisms induce bottom-up and top-down effects, and intra- (i.e. between cohorts) and inter-species interactions. The model is now fully operational for running multi-species, multi-fisheries simulations, and the structure of the model allows a validation from multiple data sources. An application with two tuna species showing different biological characteristics, skipjack (*Katsuwonus pelamis*) and bigeye (*Thunnus obesus*), is presented to illustrate the capacity of the model to capture many important features of spatial dynamics of these two different tuna species in the Pacific Ocean. The actual validation is presented in a companion paper describing the approach to have a rigorous mathematical parameter optimization [Senina, I., Sibert, J., Lehodey, P., 2008. Parameter estimation for basin-scale ecosystem-linked population models of large pelagic predators: application to skipjack tuna. Progress in Oceanography]. Once this evaluation and parameterization is complete, it may be possible to use the model for management of tuna stocks in the context of climate and ecosystem variability, and to investigate potential changes due to anthropogenic activities including global warming and fisheries pressures and management scenarios.

© 2008 Elsevier Ltd. All rights reserved.

1. Introduction

The last two decades have shown a fundamental change at the international level to address marine exploitation issues from an ecosystem perspective. However, ecosystem models adapted to an ecosystem-based management approach are at an early stage of development, and all the basic stock assessment works done by Regional Fisheries Organisations (RFOs) are still based on a species by species analytical stock assessment using population dynamics models, statistically fitted to fishing data. Ecosystem-based approach implies the integration of spatio-temporal and multi-population dynamics of at least, exploited and protected species. It requires also the consideration of interactions between populations and their physical and biological environment. These end-to-end ecosystem models should finally include a representation of the spatially-distributed effect of fisheries on the modeled population(s) to investigate impacts due to both fishing and environmental changes.

One advantage of this approach compared to the standard one currently used for stock assessment is that environmentally-constrained, spatially-explicit models allow investigation of the mechanisms that lead to observed fluctuations through the detailed spatio-temporal prediction of all age-classes. In addition, once the model parameterization is achieved for a given species, the model can be used to produce hindcast and forecast simulations to explore long-term scale variability or impacts of global warming. Taking advantage of the large fishing datasets for these

exploited species, the parameterization can be largely facilitated using data assimilation methodologies.

Briefly, models including movement and behavior of animals can be described either from a Lagrangian or Eulerian approach. While Lagrangian models focus on individual movements, the Eulerian approach considers the flux in time of density or number of individuals on a point in space. Individual-Based Models (IBMs) are typical examples of Lagrangian approach (see e.g., the model Nemuro.Fish in Megrey et al. (2007)). They can describe movement, physiology and behavior of individuals from deterministic and very detailed mechanisms, but at a high computational cost making it difficult to consider multi-species and multi-fisheries applications at Ocean basin-scale. The Eulerian approach includes the class of models based on diffusion and advection–diffusion-reaction (ADR) equations (e.g., Sibert et al., 1999). They rely on less detailed behavioral or energetic assumptions and less parameters than IBMs and appear more suited to describe population dynamics at large spatial and temporal scales. In these models the equations are numerically solved using a network of regularly spaced grid points and a discrete time step (for instance, 1° square × month). Using continuous functions, these models are also ideal for implementing parameter optimization techniques (Sibert et al., 1999; Senina et al., 2008).

The spatial ecosystem and population dynamics model (SEAPO-DYM) is an implementation of an ADR formulation that focuses on tuna spatial population dynamics. Since its early development in 1995, SEAPODYM has been continuously enhanced to provide a general framework allowing integration of the biological and ecological knowledge of tuna species, and potentially other oceanic top-predator species, within a comprehensive description of the pelagic ecosystem (Bertignac et al., 1998; Lehodey et al., 1998; Lehodey, 2001; Lehodey et al., 2003). It includes a forage (prey) sub-model describing the transfer of energy of stored biomass through functional groups of mid-trophic levels and an age-structured population sub-model of tuna predator species and their multi-fisheries. The dynamics of forage and predators are driven by environmental forcing (temperature, currents, oxygen, and primary production) that can be predicted from coupled physical–biogeochemical models.

Pursuing this development, we present here an update of the modeling approach including substantial improvements in the representation of the mid-trophic level functional groups (Lehodey, 2004) and more realistic definitions of habitats, movements, and mortality functions. Flexibility of the updated model will be illustrated with an application to two tuna species in the Pacific Ocean, skipjack and bigeye which have very different biological characteristics.

Skipjack (*Katsuwonus pelamis*) is a fast growing species, with a short lifespan (4–5 years for most of the individuals; Langley et al., 2005). They mature at an early age (9–10 months), and have relatively high natural mortality rates (Langley et al., 2005). Bigeye (*Thunnus obesus*) has longer lifespan (>10 years), older age at maturity (after 2 years), and lower natural mortality rates than skipjack (Hampton et al., 1998). They have both high fecundity and exhibit year-round spawning, though seasonal peaks are observed for bigeye. Juveniles of bigeye (*Thunnus obesus*) are frequently found together with skipjack in the surface layer, especially around drifting logs that aggregate many epipelagic species. As they become older and larger, bigeye tuna explore deeper (>600 m) layers than skipjack; the latter are usually confined to the upper mixed-layer, though occasionally able to dive below 200 m. Tuna can thermoregulate using a specialized counterflow heat exchange system (the *rete mirabile*). This system is particularly well-developed in bigeye tuna, allowing the species to have extended temperature range and hence a larger latitudinal and vertical habitat temperature. Adult bigeye tuna are thus exploited by the sub-surface long-line fishery throughout the tropical and sub-tropical oceans. As other tuna species, skipjack and bigeye have highly opportunistic feeding behavior resulting in a very large spectrum of micronektonic prey species from a few millimeters (e.g., euphausids and amphipods) to several centimeters (shrimps, squids and fish, including their own juveniles) in size. Their diets reflect their ability to capture prey at different depths and periods of the day (i.e., daytime, nighttime, and twilight hours). Thus differences in vertical behavior can be identified through detailed stomach contents analyses; e.g., adult bigeye tuna accessing deeper micronekton species (Brill et al., 2005).

While the present paper focuses on the description of new developments in the model and illustration of its capacity to capture important features of spatial dynamics of different tuna species in the Pacific Ocean, the actual validation is presented in a companion paper describing the approach to have a rigorous mathematical parameter optimization (Senina et al., 2008).

2. Modeling approach

The model domain covers the Pacific Ocean at a spatial resolution of 1° and a one-month time resolution for the period 1948–2005. Forcing fields of these simulations (temperature, currents, dissolved oxygen concentration, primary production) are provided by a coupled biogeochemical–physical ocean model that reproduces ecosystem dynamics and biogeochemical fields at seasonal to interannual time scales ((Murtugudde et al., 1996; Christian et al., 2002; Wang et al., 2005). Temperature, current, and oxygen variables are averaged in three vertical layers: epipelagic (0–100 m), mesopelagic (100–400 m) and bathypelagic (400–1000 m). They are also used to predict the biomass distributions of the six functional mid-trophic groups (Lehodey, 2004) that are potential prey of young and adult tuna and predator of their larvae.

The model simulates tuna age-structured populations with one length and one weight coefficient by cohort obtained from independent studies (see previous references and Appendix). At each time step, survival relationships describe ageing processes for the cohorts while advection–diffusion-reaction equations describe migrations, recruitment and mortality. Different life stages are considered: larvae, juveniles and (immature and mature) adults. The age structure is defined with one monthly age class for larvae, two monthly age-classes for juveniles, and then quarterly age-classes for immature (from second quarter of age to age at first maturity) and mature adults (after age at first maturity). The last age class is a "plus class" where all oldest individuals are accumulated. All temporal dynamics are computed at the time step of the simulation, i.e., one-month in the present case. Note that for simplicity, we will omit the notations of species, space and time in the following model description.

2.1. Fish thermal habitat (Φ_a)

In Holland and Brill's heat budget model of tuna (Holland et al., 1992; Brill, 1994), the difference between body temperature and ambient water temperature is shown to be linked to the whole-body heat-transfer coefficient, the rate of temperature change due to internal heat production, the ambient water temperature and the body temperature (T_b). Maury (2005) provided a more general equation of the size-dependent tuna body temperature dynamics, showing that at steady state, body temperature increases linearly with size. Similarly, it can be shown that the thermal inertia (the gradual change of the heat flux under a rapid change of the temperature gradient), is inversely proportional to the fish weight.

At the scale of a population, we consider that the thermal habitat of a given cohort (defined by an average size) can be repre-

sented by a Gaussian distribution with an average temperature linked to the size-dependent body temperature at steady state, and by a standard error of the distribution linked to the thermal inertia of the fish. Here, we assume that for a given species, there is an optimal intrinsic temperature (T_i) that remains constant, whatever the age/size, and that this temperature is a target temperature for any individual of the species (e.g., due to genetic and physiological adaptation during species evolution). It follows from the heat budget model above that when becoming larger, the fish will have to search for colder habitat temperature to compensate their increasing body temperature at steady state. But they will have also larger temperature range due to their increasing thermal inertia. Therefore, we can define a population size-dependent habitat temperature by a Gaussian distribution $N(T_a, \sigma_a)$ with linearly decreasing functions with size for T_a^* and linearly increasing function with weight for σ_a (Fig. 1).

A consequence of this definition of the species thermal habitat is that the maximal average temperature used for the Gaussian distribution occurs at age 0, i.e., spawning. We assume that the species' intrinsic temperature T_i is equivalent to the average temperature of the first cohort, i.e., that species' intrinsic temperature is defined as the optimal spawning temperature ($T_i = T_0^*$).

2.2. Feeding habitat index H_F

The feeding habitat index expresses, through a value between 0 and 1, how a particular place and time are favorable for feeding on n prey (forage) components, based on the accessibility to each of them considering both the physical ability of the predator (differ-

ent by species and by age) and the physical conditions in the water layer inhabited by the forage component. To define this feeding habitat index H_F for a given cohort a, first an accessibility coefficient ($\Theta_{a,n}$) is calculated for each forage component, based on the relationships with two critical parameters for tuna, temperature (Φ) and dissolved oxygen content (Ψ)

$$\Theta_{a,n} = \Phi_{a,n} \cdot \Psi_n \tag{1}$$

The temperature function follows a Gaussian distribution $N(T_a^*, \sigma_a)$ as described above in Section 2.1 (Fig. 1). For oxygen, a sigmoidal function is used (Fig. 2) since only minimum values constrain the accessibility to the water layer associated to the forage component:

$$\Psi_n(O_z) = \frac{1}{1 + e^{\gamma \cdot (O_z - \widehat{O})}} \tag{2}$$

with O_z, the dissolved oxygen concentration in layer z, $\widehat{O}$, the oxygen value for $\Psi = 0.5$ and γ, a curvature coefficient. For prey components that migrate at night to upper layers with different physical conditions, we calculate the mean temperature and oxygen concentration weighted by the day and night length. The feeding habitat index for n forage (F) components is then:

$$H_{F_a} = \sum_n \Theta_{a,n} \frac{F_n}{F_{max}} \tag{3}$$

and F_{max} is used for standardizing F between 0 and 1.

2.3. Spawning habitat index H_S

A spawning habitat index (H_S) is used to constrain the spawning success to environmental conditions and to drive the movement of mature fish towards favorable spawning grounds. Spawning habitat and larvae dynamics are defined to represent four mechanisms that are assumed to control the survival of larvae and the subsequent recruitment:

(1) changes in the spatial extent of the spawning habitat with temperature;
(2) coincidence of spawning with presence or absence of food for larvae, i.e., the match/mismatch mechanism proposed by Cushing (1975);
(3) coincidence of spawning with presence or absence of predators of larvae;
(4) redistribution of larvae by the oceanic circulation that can create retention of larvae in favorable areas with lower natural mortality or conversely move the larvae in unfavorable zones where the natural mortality will be higher.
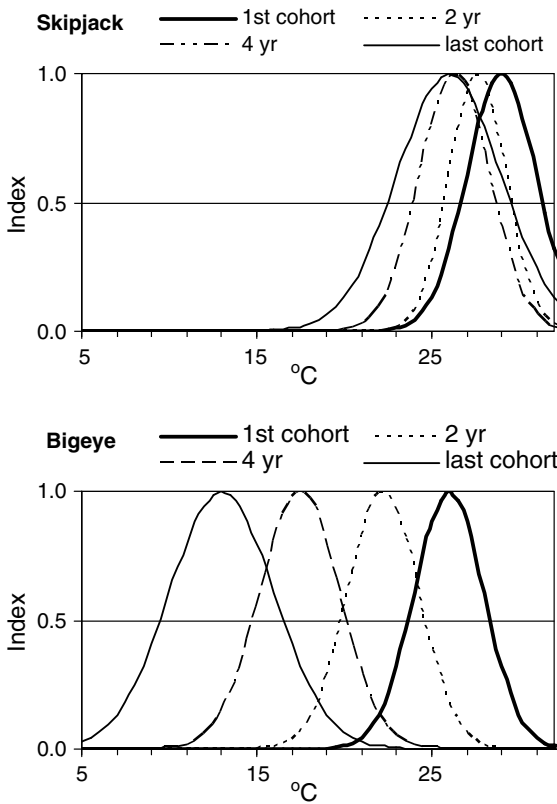

Fig. 1. Change in temperature function used to define the habitat temperature of the population based on a Gaussian distribution with linearly decreasing average temperature with size and increasing standard error with weight. Example of parameterization used for skipjack and bigeye. The average size of the latest cohort for these two species is 80.15 cm and 175.08 cm, respectively, with corresponding weights of 10.61 kg and 113.93 kg.
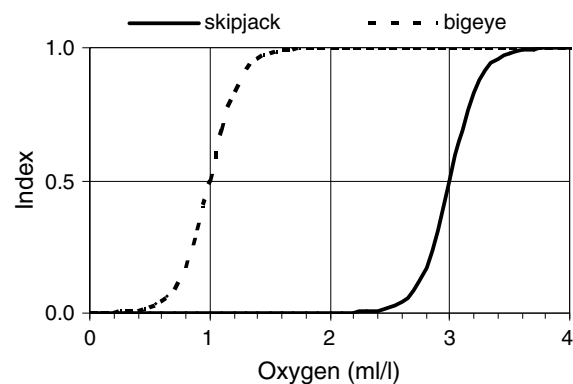

Fig. 2. Change in oxygen function used to compute accessibility coefficient to forage components. Example of parameterization used for skipjack and bigeye.

Thus H_S is given by the following equation with $\Phi_0(T_0)$, the spawning temperature index in epipelagic layer (see above), and Λ, the ratio between food abundance of larvae (micro-zooplankton approximated by primary production) and predator density of larvae, i.e., the sum of biomass of mid-trophic groups present in the epipelagic layer during day-time and sunrise and sunset periods:

$$H_S = \Phi_0(T_0) \cdot \frac{\Lambda}{\alpha + \Lambda} \tag{4}$$

The amplitude of the trade-off effect between food and predator of larvae is proportional to a coefficient α, so that if $\alpha = 0$, only temperature has an effect on the spawning, while the trade-off effect between densities of food and predators increases relative to the temperature effect with increasing α. Finally, the number of larvae recruited in each cell of the grid at a given time is the product between H_S and a number R_S, with the primary condition that adult fish, i.e., potentially mature, are present in this cell. R_S can be fixed or linked to the adult spawning biomass, e.g., with a Beverton–Holt relationship. After spawning, currents in the surface layer redistribute larvae, and a natural mortality coefficient is applied before entering in the juvenile cohorts.

2.4. Movement

In the model, surface currents passively transport tuna larvae and juveniles, while young and adult tuna can direct their own movements, in addition to being advected by currents. For both types of movements, the displacement per time unit is obviously directly dependent on the size of the individuals. Therefore, for a given size, the movement is linked to a maximum sustainable speed (V_M) expressed in Body Lengths per second. V_M can be defined as the average speed that an individual can maintain for a long period of time (e.g., over several days). In addition, we can expect that individuals will tend to stay longer in the presence of favorable conditions (low diffusion) but will want to escape quickly from unfavorable habitats (high diffusion), so that diffusion values should be linked to habitat condition. Finally there is a trade-off between advection and diffusion, which can be stipulated according to a few realistic hypotheses. They are best illustrated with extreme conditions (see Table 1):

1. if habitat is null and there is no gradient, all displacement is due to diffusion with individuals escaping at V_M in any straight-line direction. Population diffusion is maximal and there is no advection;
2. if habitat is null and there is a maximum positive gradient, there is (almost) no diffusion and advection is maximum (positive in sign);
3. if habitat is maximal and there is no gradient, all displacement is due to diffusion, but the diffusion is low since individuals stay in this favorable area: there is (almost) no diffusion and no advection;
4. if habitat is maximal and there is a maximum negative gradient: there is (almost) no diffusion and advection is maximum (negative in sign).

For directed movements, we assume that V_M is the maximal sustainable speed of fish, which can be reached when the gradient of the habitat (standardized between 0 and 1) is maximal (G_{max}). The taxis coefficient χ is then given by equation:

$$\chi_a = \frac{1}{G_{max}} \cdot V_M \cdot l_a \tag{5}$$

with l_a being the fish size (fork length) in cohort of age a, and G_{max}, the maximum gradient of the standardized habitat. Fig. 3 illustrates the change of advective movement according to size and habitat gradient.

The total advection (A) is the algebraic sum of movements due to currents and directed displacement (taxis):

$$A_x = u + \chi \cdot G_x \tag{6}$$

with u, the zonal current and G_x, the gradient of habitat index in the x-direction (in the y-direction, v, the meridional current, and G_y replace u and G_x).

For movement by diffusion, assuming that fish are moving according to simple (isotropic) random walk in two-dimensional space (i.e. purely diffusively), the diffusion coefficient D_{max} can be expressed as $D = V^2 t/4$ (see, for example, Okubo (1980)), with V, the maximal speed (equals to $V_M \cdot l$) and t being the computational time unit. This value is purely theoretical and does not consider many factors which make animal dispersal biased in the natural habitat. This maximum value decreases with the habitat index I, and the trade-off between diffusion and advection is introduced with the term $(1-0.9\rho)$, where ρ is the ratio (in absolute value) between the current gradient value and the maximal gradient G_{max}. The factor 0.9 is added to avoid zero diffusion and therefore prevent numerical instabilities in the PDE solver being used. Finally, the equation of diffusion D in relation to the body size, the habitat value, and the gradient is given as:

$$D(N) = D_{max} \cdot \left(1 - \left[\frac{I}{c+I}\right]\right) \cdot \left(1 - 0.9 \cdot \left|\frac{G}{G_{max}}\right|\right) \tag{7}$$

with c, a curvature coefficient. We can verify that using this definition, the changes in diffusion with habitat and its gradient agree with extreme conditions as summarized in Table 1. We were also interested in testing the effect of population heterogeneity on the diffusion coefficient, i.e., in linking D to the density of the population N, which is accounted for by multiplying D_{max} by the term $[1 - e^{(-\eta N)}]$, with $\eta > 0$. All movements, both advection and diffusion, are therefore linked to
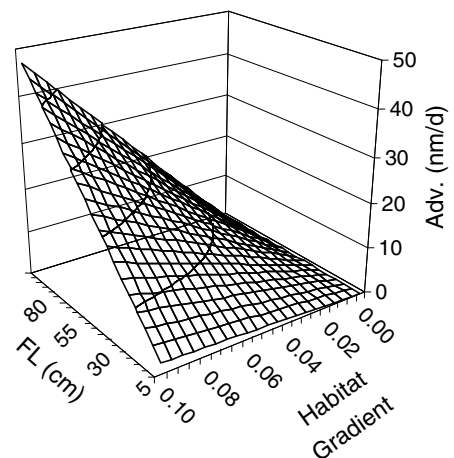
Table 1
Advection (A) and diffusion (D) terms in extreme conditions of habitat (I) and habitat gradient (G), using Eq. (5)

I	G	D	A
0	0	D_{max}	0
0	G_{max}	0	V_M
1	0	~ 0	0
1	$-G_{max}$	0	V_M

Fig. 3. Change in taxis coefficient χ (nautical miles day^{-1}) in relation with body size (l) and habitat gradient (with $V_M = 1$ body length s^{-1}).

body size and habitat and defined by three parameters (V_M, c and η), or only two if density dependence is not included.

2.5. Spawning and feeding migrations

The emergence of optimal seasonal spawning grounds is the result of natural selection and evolution of the species that need to optimize reproductive efforts for the survival of the offspring under the constraints of environmental variability. For many species, the seasonal cycle of reproduction and its associated maturation process is believed to be controlled by strong seasonal factors, e.g., changes in temperature and light (day length or its gradient, e.g., Okamura, 2008). Trying to reproduce the seasonal change between feeding and spawning migrations, we made the following assumptions:

(i) with the nearing of the seasonal spawning period, adult tuna tend to direct their movements to locations with similar environmental conditions as those during their own birth, i.e., we postulate as Cury (1994), that "a newborn individual memorizes early environmental cues, which later determine the choice of its reproductive environment. Thus, the same mechanism accounts for successive generations reproducing at the same geographic location (philopatry) or aiming at a moving target, i.e., a set of environmental conditions that do not always have the same earth coordinates (dispersal)";
(ii) these conditions are defined by the spawning habitat index H_S;
(iii) the seasonal effect is controlled by the day length and by its gradient (i.e., varying with latitude);
(iv) the triggering effect for switching from the feeding habitat to the spawning habitat is linked to a threshold in the rate of increase of the day length.

Using a function based on the day-length, it is easy to change the directed movement according to either the feeding or the spawning habitat index. This switch occurs earlier for (mature) fish that are in higher latitudes, and therefore far from their spawning grounds in warm waters (Fig. 4). Note that in low latitudes, the gradient of the day-length is too low to have any effect and adult habitat is always driven by the feeding habitat, leading in that case to opportunistic reproduction.

Practically, the habitat index (I_a) controlling the movements is always the feeding habitat index for immature adult fish, but can switch seasonally from feeding to spawning index for mature fish following Eq. (8) below and illustrated in Fig. 5
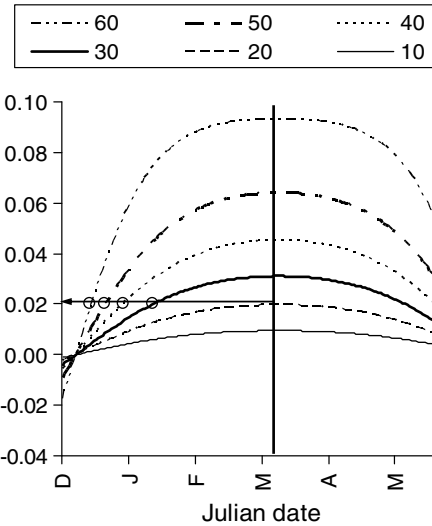

Fig. 4. Example of seasonal cycles in gradient of day length at different latitudes in the North hemisphere. With a threshold set above 0.02 h per day, the adult habitat that constrains the movement of fish will switch from feeding habitat to spawning habitat after mid-December for mature fish at latitude 60°, and one-month later at latitude 30°. Movements of fish at latitudes below 20° remain always driven by the feeding habitat.

$$I_a = H_S \cdot \frac{1}{1 + e^{\kappa \cdot (G_d - \widehat{G_d})}} + H_{F,a} \cdot \frac{1}{1 + e^{\kappa \cdot (\widehat{G_d} - G_d)}} \qquad (8)$$

with G_d, the gradient of day-length, $\widehat{G_d}$, the threshold in the gradient of day-length at which the switch occurs and κ, a curvature parameter.

Since feeding and spawning habitats can have opposite characteristics (high forage biomass and relatively low temperature for feeding, but low forage biomass, i.e., larvae predators, and higher temperature for spawning), this definition can potentially lead to drastic changes in the movement of fish feeding in high latitudes at the time of spawning migration; a behavior that has been successfully observed for example for bluefin tuna tagged with electronic tags (Block et al., 2005).

2.6. Food requirement index

Though the feeding habitat H_F used to constrain the movement of fish results directly from the spatio-temporal distribution of prey species, it does not include a direct link between the available
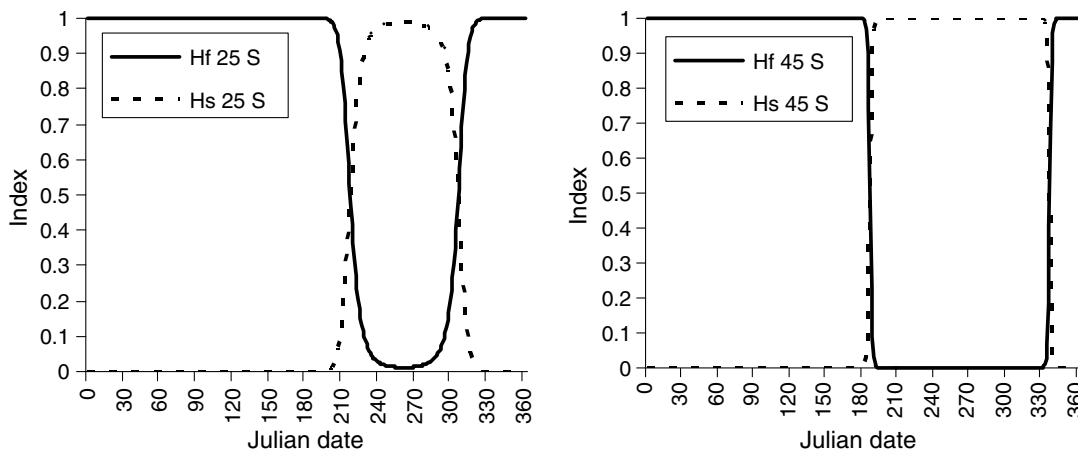

Fig. 5. Examples of switches in the contribution of feeding and spawning indices to the adult habitat index (Eq. (8)) at latitude 45°S and 25°S based on a threshold of 0.02 h per day ($\kappa = -1000$).

biomass of prey (forage) and the food requirement of the predators (tuna), especially since oriented movements are based on the gradient of the habitat index, not on absolute values. In this version of the model, we have revised this aspect of the prey–predator relationship through the definition of a food requirement index $I_{FR,a}$ that is used to adjust locally the natural mortality of the species, based on intra- and inter-species competition.

For a given cohort of any of the predator species, we want to calculate I_{FR} with the following conditions: the index should be linked to the total forage requirement by all explicitly described predator populations (sum by cohort) as well as to the relative contribution to this total food requirement by the cohort considered. This index will vary from 0 (high contribution to a total forage requirement that is much higher than available forage) to 1 (low contribution to a total forage requirement that is much lower than available forage).

To compute I_{FR}, first we need to compute the total forage requirement for each component n (F_{Rn}) which is the sum of contributions from all cohorts (a) of predators (sp) $F_{Rn,sp,a}$:

$$F_{Rn} = \sum_{sp,a} F_{Rn,sp,a}$$

where

$$F_{Rn,sp,a} = (N_{sp,a} \cdot w_{sp,a} \cdot r_{sp} \cdot \vartheta_{n,sp,a}) \cdot t \tag{9}$$

with r, the average daily food ration, w, the weight-at-age coefficient and $\vartheta_{n,sp,a}$ the relative accessibility coefficient:

$$\vartheta_{n,sp,a} = \frac{\Theta_{n,sp,a}}{\sum_n \Theta_{n,sp,a}} \tag{10}$$

We can define, for each forage component n, a measure of the total forage requirement relative to the forage available F_n, i.e., the total forage mortality ω due to all predator cohorts:

$$\omega_n = \frac{F_{Rn}}{F_n} \tag{11}$$

and the partial contribution to this value by each predator cohort:

$$\omega_{n,sp,a} = \frac{F_{Rn,sp,a}}{F_n} \tag{12}$$

The index $I_{FR,sp,a}$ combines both the total and the partial measures of forage mortality rates, i.e., the product $(\omega_n \cdot \omega_{n,sp,a})$ to account for the effects due to all predators cohorts together as well as the specific cohort for which the index is computed. Finally, the index $I_{FR,sp,a}$ is the sum over the n components of this product, standardized between 0 and 1 using the function $f(x) = 2^{-x}$:

$$I_{FR,sp,a} = 2^{-\rho \sum_n \omega_n \cdot \omega_{n,sp,a}} \tag{13}$$

2.7. Natural mortality

Average natural mortality by age $M_{sp,a}$ in the population (Fig. 6) is described as the sum of two functions (Eq. (14)). An exponentially decreasing function with age represents the mortality during the early life history (mainly due to starvation and predation). An increasing function with age characterizes natural mortality in the adult phase, i.e., mainly senescence and diseases.

$$M_{sp,a} = \left[M_{P_{max},sp} \cdot e^{(-\tau_1 \beta_P)}\right] + \left[M_{S_{max},sp}/(1 + e^{\beta_S \cdot (\tau - A_{0.5})})\right] \tag{14}$$

with $M_{P_{max},sp}$ and $M_{S_{max},sp}$, the maximal mortality values of predation and senescence functions, β_P and β_S, the slope coefficients, and $A_{0.5}$, the age at which 1/2 of $M_{S_{max},sp}$ occurs.

The average natural mortality-at-age coefficients $M_{sp,a}$ can be modulated in space and time based on local conditions expressed through any standardized index I between 0 and 1. We use a simple linear relationship:
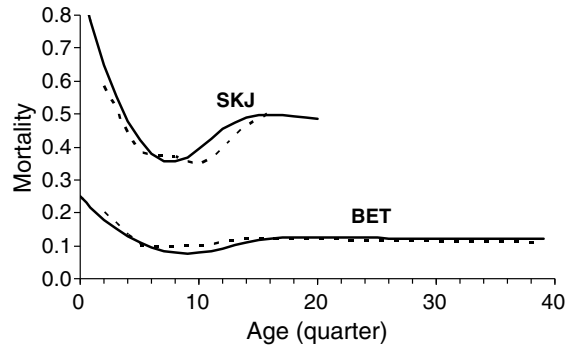

Fig. 6. Average natural mortality coefficient by age for skipjack and bigeye tuna used in the present study (thick black curves). Parameters of the mortality functions (see Appendix) were fitted to obtain close values from those (dotted lines) estimated with the stock assessment model MULTIFAN-CL (Langley et al., 2005; Hampton et al., 2006).

$$M_{sp,a,i,j} = M_{sp,a}(1 - I_{i,j} + \varepsilon) \tag{15}$$

where the local natural mortality coefficient is lower than average value if the index is above ε and higher if below ε. The food requirement index I_{FR} calculated for immature and mature adults is used, allowing us to take into account a competition effect between cohorts and between species.

3. Results

Our aim in this study was to illustrate the capability of the model to reproduce a large range of realistic spatio-temporal dynamics using test simulations with a plausible parameterization defined for two tuna species, skipjack and bigeye tuna (cf. Appendix), both from the literature review and the parameter optimization method described in the companion paper (Senina et al., 2008).

3.1. Spawning habitat

The distribution of spawning habitat predicted for the two species is shown in Fig. 7 for two different months. The parameterization differs between species through the optimum spawning temperature, 28 °C and 26 °C for skipjack and bigeye, respectively, and the value of the α larvae food–predator trade-off coefficient, increasing from 1 for skipjack to 3 for bigeye. These simple changes in parameterization create very different patterns in spatial distribution of the spawning index, with reasonable comparison to observed concentration areas of larvae (Fig. 7c). Based on this spawning index, the final larval distributions (Fig. 7d) also integrate the presence of mature fish for spawning and the drift due to currents in the surface layer. The model produces highly dynamic predictions of larval distributions that include shifted peaks in different regions of the Pacific and interannual (ENSO) changes with abundance increases during El Niño events (Lehodey et al., 2003). Additionally, it also shows stable patterns like seasonal peaks in the northern and southwestern tropical regions during summer, and relatively constant favorable areas, e.g., Philippines–Indonesia regions for skipjack, or the central Pacific and a portion of the Kuroshio between Taiwan and Okinawa Islands for bigeye.

3.2. Feeding habitat

The physical constraints due to temperature and oxygen for skipjack and bigeye are illustrated in Fig. 8. Average values are presented for skipjack in the surface layer and for bigeye in the mesopelagic layer, because this latter species is known to spend a large
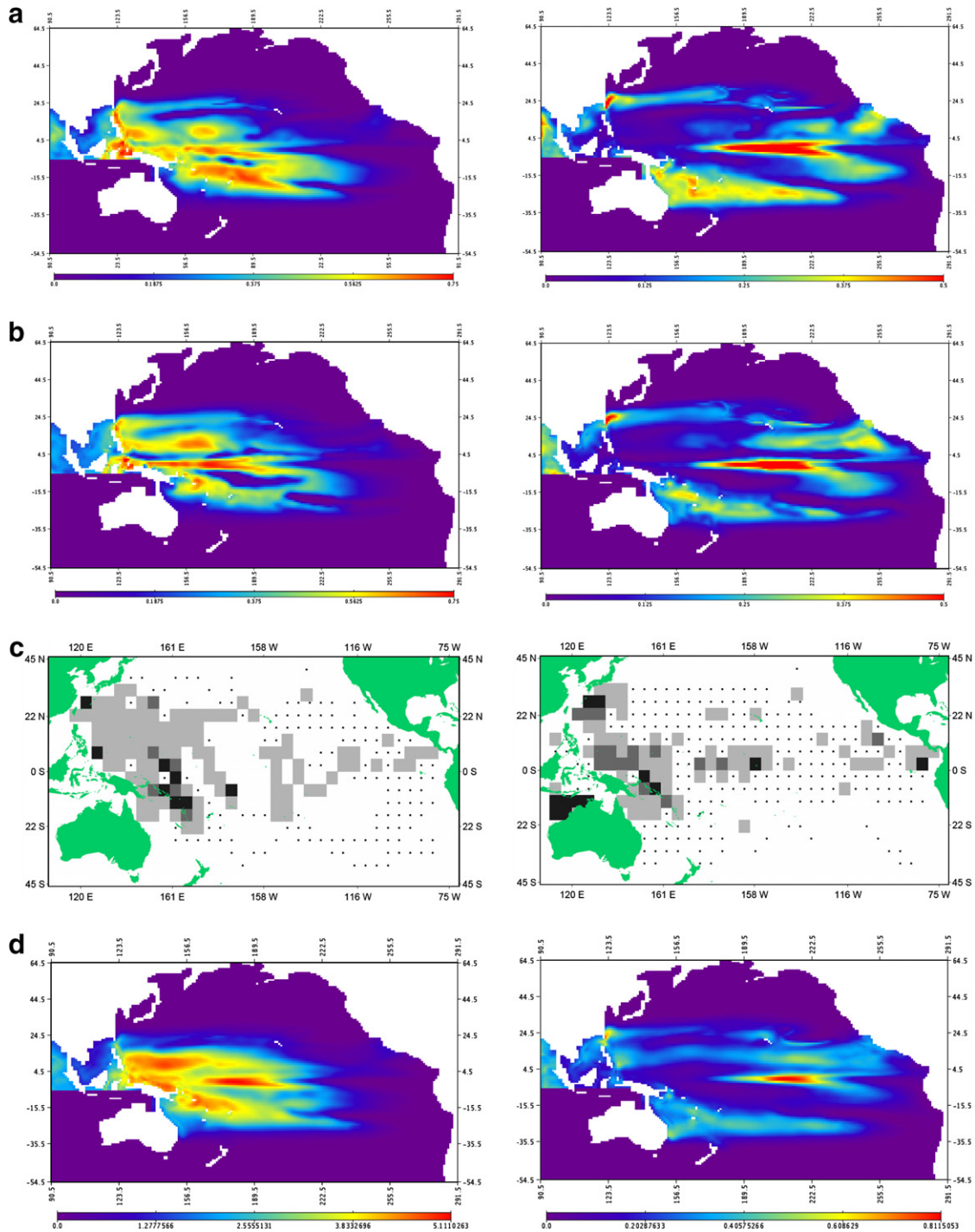
Fig. 7. Predicted distribution of the spawning index in January (a) and July (b) 2004 for skipjack (left) and bigeye (right) larvae in the Pacific Ocean, and comparison between (c) observed densities of larvae (redrawn from Nishikawa et al., 1985) and (d) predicted average annual distribution of larvae for each species, respectively. Density of larvae in (c) increases from grey to black, while dots indicate no larvae in the sampling.

part of its time in deep layers. The temperature index is given for one cohort corresponding to a size of 45 cm and 105 cm for skipjack and bigeye respectively since as described above, the habitat temperature changes with size/age (see Section 2.1). Though oxygen requirement is likely to also change with age, we use a constant parameterization with age in the absence of detailed information. Based on experimental evidence, tolerance of skipjack to low dissolved oxygen concentration is known to be much lower than for bigeye, and while dissolved oxygen concentration in the range 0.5–1.0 ml l^{-1} seems to be a limit for bigeye (Sharp, 1978;

Sund et al., 1980), values above 2–3 ml l^{-1} are needed for skipjack (Brill, 1994). We therefore used the values 3 and 1 ml l^{-1} to parameterize the oxygen function for skipjack and bigeye, respectively.

The superimposition of oxygen habitat index isopleths on the habitat temperature index for the selected cohort (Fig. 8a) shows a wide region (35°N–35°S) of favorable habitat temperature in the surface layer for skipjack where oxygen is not a limiting factor except in the far eastern Pacific. In the sub-surface layer, very low oxygen concentrations also create unfavorable conditions for bigeye, despite its better tolerance to lower concentration. But this
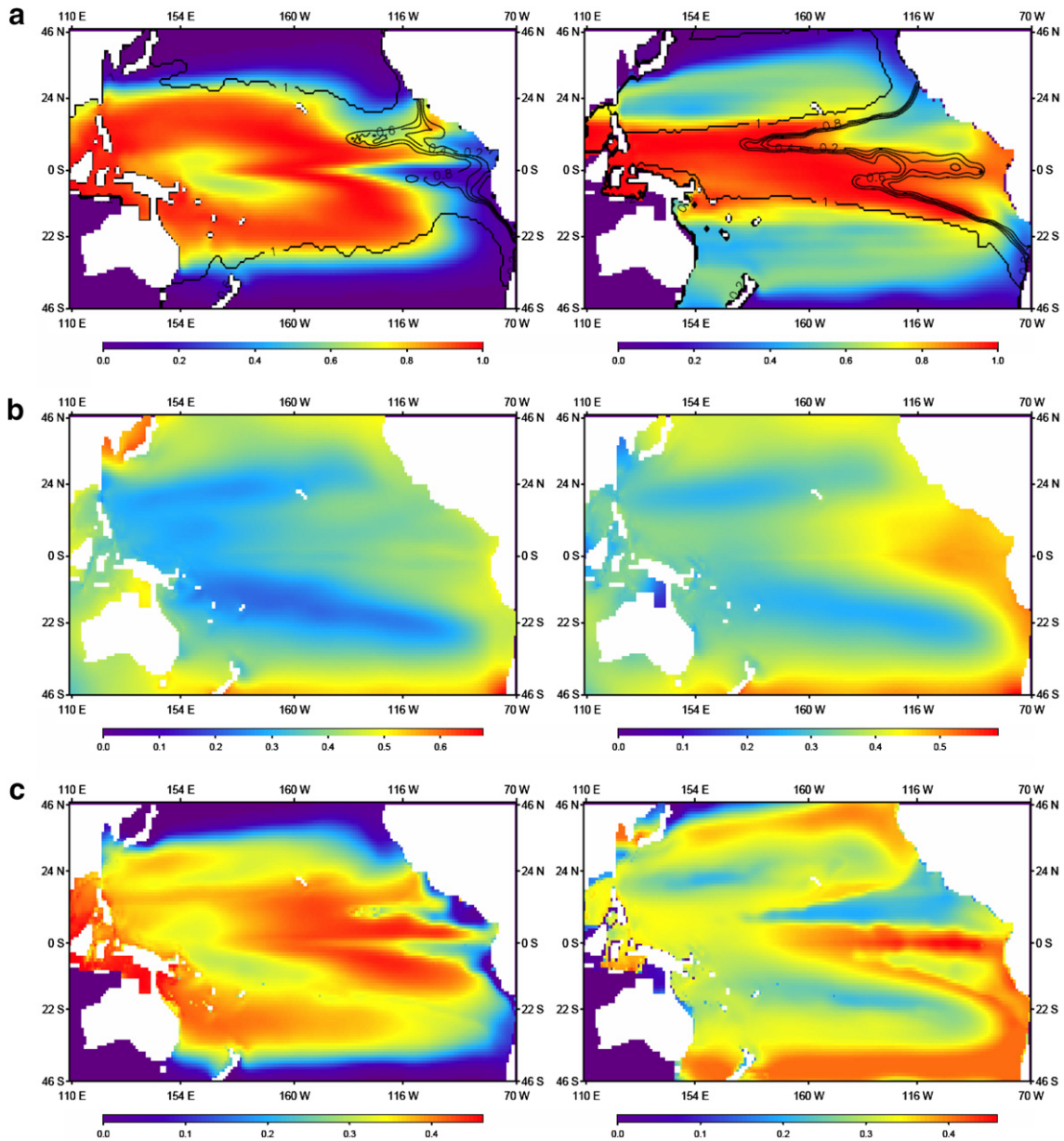
Fig. 8. Average distributions of (top) temperature index on which are superimposed isopleths of oxygen index for skipjack (left) and bigeye (right); (middle) daytime biomass (g m^{-2}) of epipelagic (left) and mesopelagic (right) mid-trophic functional groups (Lehodey, 2004), and (bottom) feeding index for skipjack (left) and bigeye (right) based on the different abilities by the species to access the different mid-trophic groups (i.e., prey) according to temperature and oxygen conditions.

is not the case in the surface layer. Bigeye (of the selected size range) have a very favorable sub-surface habitat temperature between 20°N–20°S all across the Pacific Ocean and still relatively favorable habitat values extending to latitudes of 40°N and S. Of course, bigeye can also compensate unfavorable habitat in sub-surface by increasing the time spent in the surface layer.

The feeding habitat as defined above (Section 2.2) integrates the accessibility to different mid-trophic groups, i.e., forage (Fig. 8b), based on the temperature and oxygen constraints in the vertical layers. On average, favorable feeding habitats (Fig. 8c) occur in the central and south-eastern equatorial Pacific for both species, and in the far western (Philippines–Indonesia), especially for skipjack. Despite high values of feeding habitat, it should be noted that skipjack does not enter the very shallow waters like in the Torres Strait (<20 m) and the Gulf of Carpentaria (<80 m). During summer, favorable feeding habitats occur in the western sub-tropical regions for skipjack and in the southern and northern sub-tropical

convergence zones for bigeye. However, predicted interannual variability due to ENSO strongly disrupts such an average spatial pattern.

Another interesting approach to analyzing the feeding habitat is to compute the proportion of each mid-trophic group entering the predicted diet of the predator. This allows comparisons with multiple stomach contents analyses. Given the level of potential details predicted by the model, i.e., biomass of each cohort at a given time and position, we aggregated the data through a few regions and compared average values for young and adult fish (Fig. 9). Overall, there are limited changes for skipjack considering regions or life stages. The diet is dominated by epipelagic group (~2/3), then migrant mesopelagic and highly-migrant bathypelagic groups which are the organisms present in the epipelagic layer between sunset and sunrise. Nevertheless, in the western central tropical ocean where sub-surface waters are still warm and well-oxygenated, the adult skipjack diet also includes low proportions of mesope-

lagic or bathypelagic organisms migrating in the mesopelagic layer at night.

For bigeye, the diet is more variable between young and adult fish and regions. The diet of young fish is dominated by non-migrant mesopelagic species in the west, by migrant-mesopelagic in the north-east, and by equal proportions of both migrant and non-migrant mesopelagic species in the east. Other significant contributions in the diet of young fish come from the epipelagic group in the eastern Pacific, and from the migrant bathypelagic group. When they are adult, bigeye can access to all forage components except in the coldest north-east region where they cannot access the meso- and bathypelagic layer.

3.3. Movement

The comparison of average spawning (Fig. 7d) and feeding (Fig. 8c) habitat distributions shows that for skipjack, favorable spawning habitat index occurs on average in the western central tropical Pacific Ocean (20°N–20°S) but the highest feeding index is in the eastern and sub-tropical regions. For bigeye, with the notable exception of the area in the equatorial central Pacific, spawning and feeding indices are also spatially shifted, with

favorable feeding grounds in the eastern Pacific and at high latitudes. As a result, the predicted average biomass distribution of fish biomass (Fig. 10) is quite different from both habitat indices.

It is also obvious that seasonal to interannual variability can lead to drastic changes in the movements and spatial distribution of fish. Fig. 10 illustrates the changes in movements and spatial distribution of fish due to ENSO variability. Predicted movements of skipjack during El Niño events show strong eastward directed displacement in the equatorial region, in good agreement with observations from catch and tagging data (Lehodey et al., 1997), and westward movement on either side of this equatorial band. The diffusion is maximal in the southern sub-tropical gyre where feeding index is very low (Fig. 8c). In the reversed La Niña situation, skipjack move to the west of the equatorial region and diffusion increases in the northern sub-tropical gyre where biomass of epipelagic micronekton reaches a minimum.

For bigeye tuna in general, predicted movements encompass a range of lower advection and diffusion values than those observed for skipjack. This is likely because bigeye can access meso- and bathypelagic groups of prey, thus areas of very poor feeding habitat
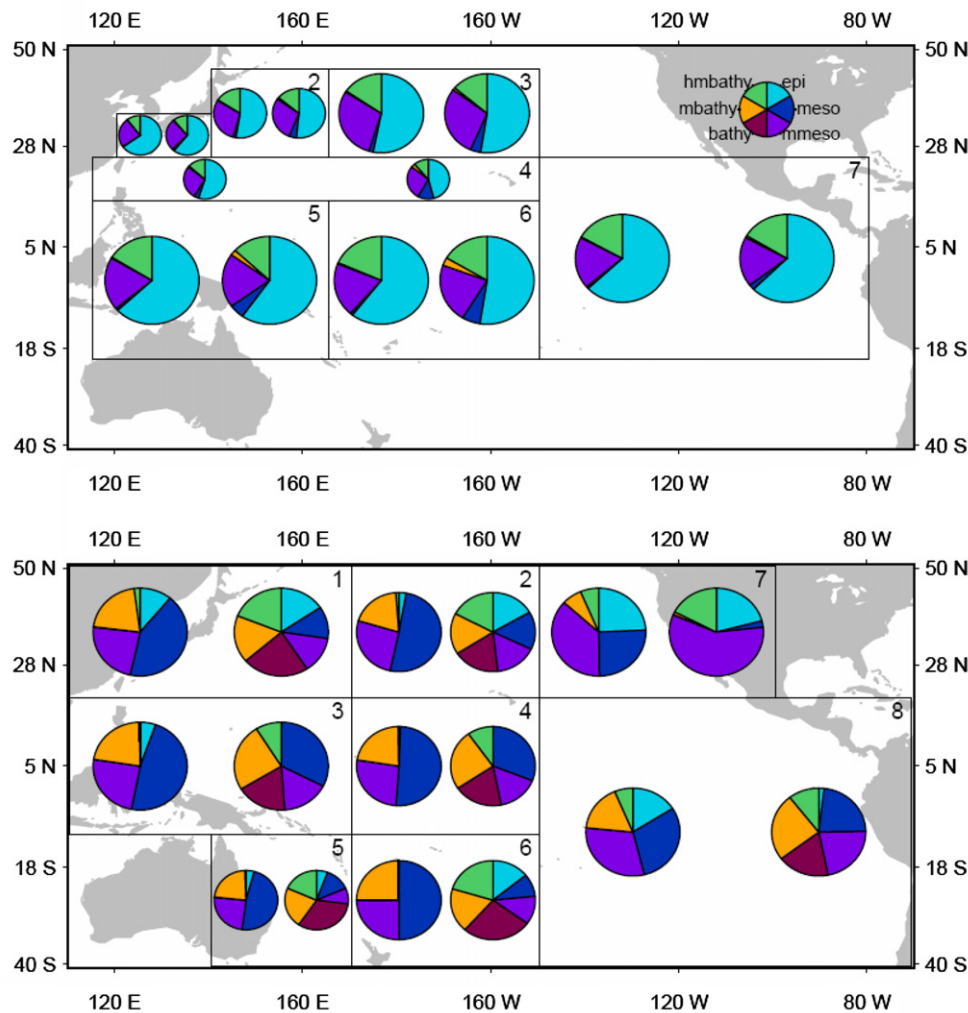

Fig. 9. Average proportions of mid-trophic groups entering in the predicted diet of skipjack (top) and bigeye (bottom). Data are aggregated over 10 years (1995–2004) in sub-regions following a stratification based on fishing data used for stock assessment analyses (Hampton et al., 2006). There are two pie-plots by region for young immature (left) and adult mature (right) fish. The mid-trophic sub-model (Lehodey, 2004) includes six functional groups in three vertical layers: epi, epipelagic; mmeso, migrant mesopelagic; meso, non-migrant mesopelagic; mbathy, migrant bathy-pelagic; hmbathy, highly-migrant bathypelagic; bathy, non-migrant bathypelagic.
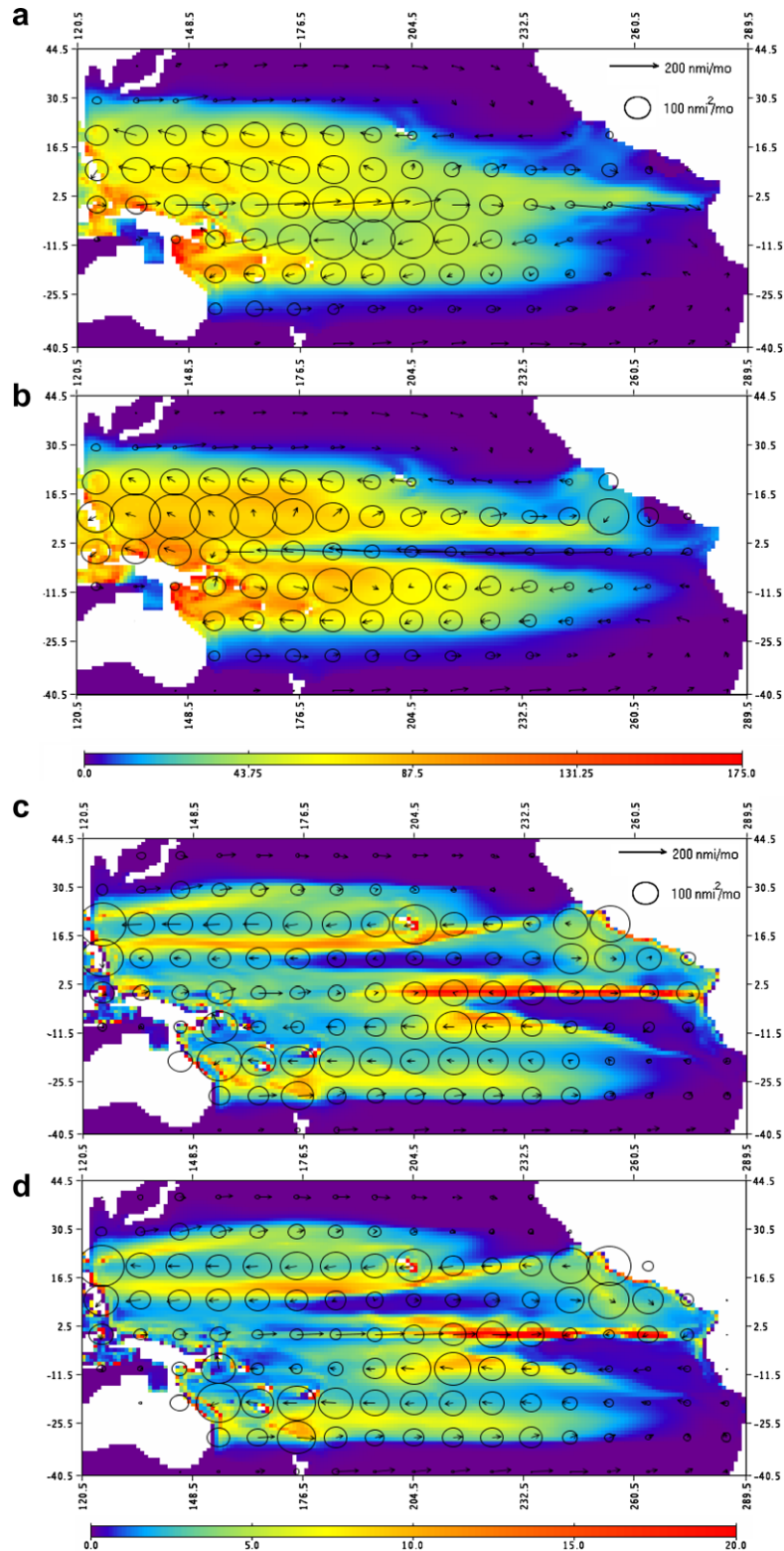
Fig. 10. Distribution of biomass of skipjack (a,b) and bigeye (c,d) cohort at first month after age of maturity in November 1997 (a,c: El Niño phase) and November 1998 (b,d: La Niña phase) in the Pacific Ocean. Circles and arrows represent random (diffusion) and directed (advection) movements of population density correspondingly and averaged by 10° squares.

for this species are less frequent and present weak gradients. The model predicts a zone of concentration in the equatorial band east of 150°W where relatively high diffusion values can be observed despite a good habitat, but due to the density effect associated with a high concentration of fish.

3.4. Food competition

The last mechanism investigated in the present analysis was the potential interaction between species through changes in natural mortality due to the food requirement index. As

described above (Section 2.6), this index provides a relative measure of food competition between cohorts of all predator species explicitly represented in the model. The results of a multi-species simulation, i.e., with skipjack and bigeye together, were compared to those of two separate single-species simulations for the recent period 1980–2005 (Fig. 11). The parameter ε
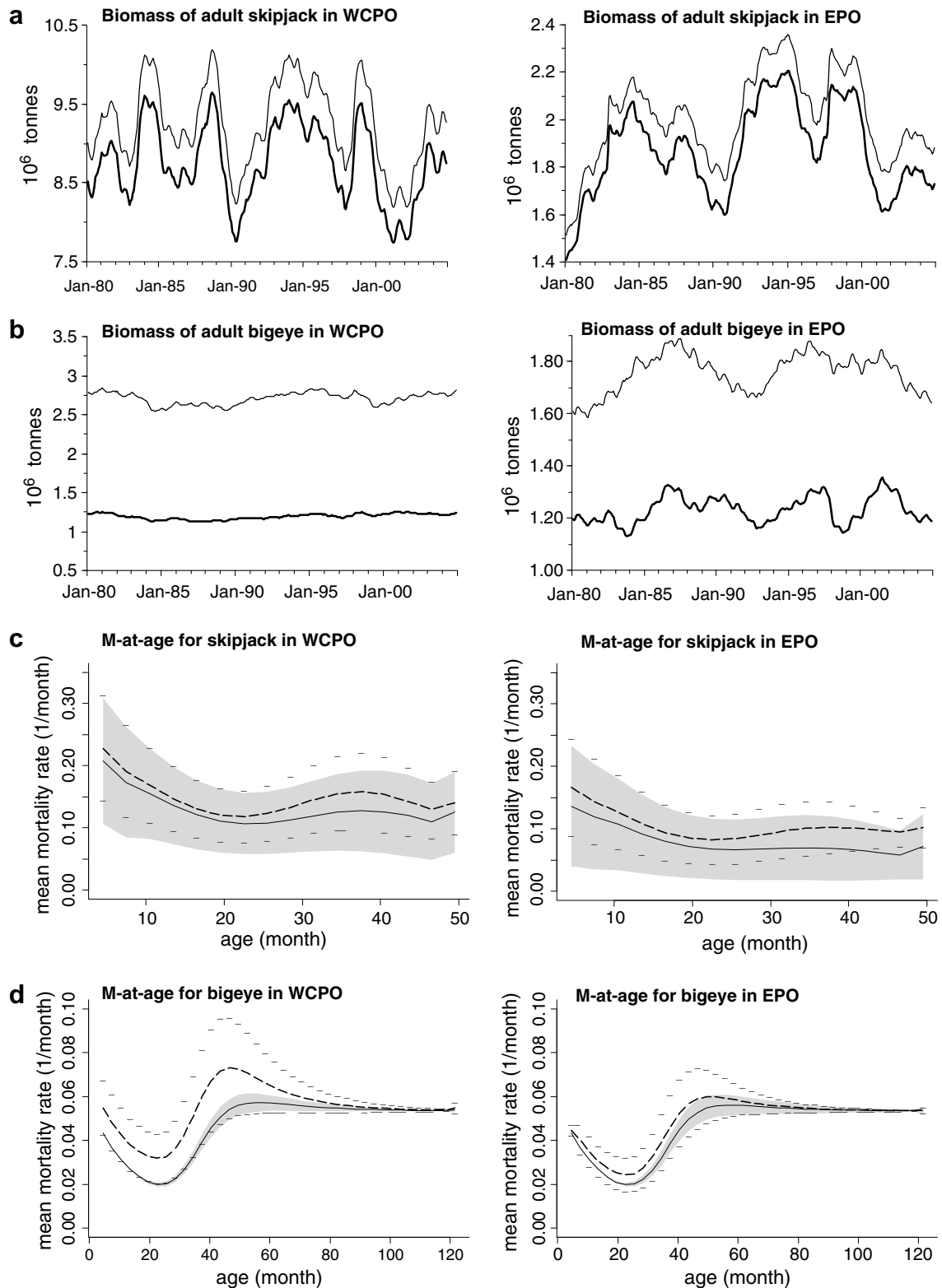
Fig. 11. Time series of biomass of adult skipjack (a) and bigeye (b) comparing single (thin curves) vs. multiple (thick curves) species simulations in the western–central (WCPO) and eastern (EPO) Pacific Ocean (using longitude 150°W as a boundary between the two regions), and corresponding average and standard errors of mortality by age modified by the food requirement index I_{FR} for skipjack (c) and bigeye (d). Thin curves and grey shaded area are for single-species simulation and dotted curves are for multi-species simulation. Note that fishing mortality is not included in these simulations.

(Eq. (15)) was set to 0.5, which means that mortality defined by Eq. (14) is lower when food requirement index I_{FR} is above 0.5 and higher when I_{FR} is below 0.5.

For skipjack, there is a slightly lower biomass ($\sim-5\%$) in the case of the two-species simulation in both WCPO and EPO. For bigeye however, the decrease is much higher with a 25% biomass reduction in the EPO and 57% in the WCPO. The very large biomass of skipjack has logically a strong impact on bigeye cohorts through food competition, especially in the WCPO which is the core habitat of skipjack. When computing the mortality coefficients over the two east and west regions by age resulting from Eq. (15) (Fig. 11), we obtain effectively higher average mortality rates in the case of the multi-species simulation, with higher intensity in the WCPO than in the EPO. But these curves also indicate that this interaction occurs more strongly between the oldest cohorts of skipjack and the youngest cohorts of bigeye. In growing older, bigeye access deep forage components that are not available for skipjack (Fig. 9) and thus the mortality effect due to food competition gradually decreases (Fig. 11).

4. Discussion

The model SEAPODYM has been upgraded to include more detailed relationships between population dynamics and basic biological and ecological functions, including a more realistic representation of the vertical oceanic habitat, both in terms of physical and foraging conditions. On the other hand, because this model is aimed to be used for ecosystem-based management, we attempted to keep the number of parameters to a minimum to facilitate formal parameter optimization required for assessment analyses. The habitat-based approach used here facilitates this parameterization since it allows combining several mechanisms to consider relative effects (e.g., the ratio between prey and predator densities of larvae) instead of absolute values of parameters, that are often difficult to measure (e.g., the natural mortality rate of larvae) and to evaluate.

Because the model is driven by the bio-physical environment of the ecosystem, it was possible to reduce the number of parameters that describe the complete spatially-explicit population dynamics of a species to 21 (cf. Appendix), i.e., a small number relative to the number of variables described in the model. A few more parameters should be added to include the growth function that is still provided by independent studies in this version. Other parameters (not detailed here) concern the description of fisheries (selectivity and catchability), since the model includes a full description of multiple-fisheries and predicts catch and length frequency of catch (Bertignac et al., 1998; Lehodey et al., 2003).

Fishing data is critical to evaluate the outputs of the model, and make possible the discrimination between changes in catch and population that are attributed either to the fishing activity or to the climate-related variability (e.g., ENSO). Extending beyond a simple comparison of results between predicted and observed catch, this fishing information can be used to optimize the parameterization by implementing a statistical procedure directly in the model. This approach has been developed using the maximum likelihood and adjoint techniques and tested with an application to skipjack tuna (Senina et al., 2008), that yields promising results. Once the best parameterization of the model is obtained and the predicted results fully evaluated, it may be possible to use this model for many different management scenarios taking advantage of its spatial multi-species multi-fisheries structure. In a future version, parameter optimization should also benefit from the use of conventional tagging data (e.g., Sibert et al., 1999) that would bring significant additional information for estimating several critical parameters (e.g., movements, habitats, recruitment and mortality).

Another attribute of the model compared to standard population assessment models (e.g., Hampton and Fournier, 2001; Maunder and Watters, 2003), is that the predictions are sufficiently detailed to allow quantitative comparisons with data other than catches. There exists a large diversity of observations collected over the previous decades for exploited tuna and tuna-like species. The model can offer a simple framework to compare the numerous diet studies that have been carried out in many different regions during several decades (e.g., King and Ikehara, 1956; Bertrand et al., 2002). At the same time, it provides accurate habitat prediction (in time, space and for a given age) that can be used to investigate detailed individual behaviors as observed from electronic archival tags (e.g., Schaefer and Fuller, 2002). Temperature data recorded by these tags can help to evaluate and parameterize the proposed thermal habitat, and depth records compared to predicted fractions of the time spent in different layers during day and night. These tags also can provide independent estimates of maximum sustainable speed by age. Predicted distributions of larvae can be compared to the past observations collected during sampling cruises, and may in the future be used to plan or even optimize new ones in real-time, e.g., to check particular areas predicted to be highly favorable.

The present study shows that the model can produce realistic habitats and dynamics for two tuna species based on coherent and limited changes of a few parameters, i.e., essentially those defining the spawning and feeding habitats. It demonstrates also how complex patterns emerge from simple mechanisms embedded in a highly dynamic environment. The case of tuna is particularly interesting since the different species cover a large range of habitats with different biological characteristics, from species with warm water affinities and short lifespan to species with colder water affinities and long lifespan, i.e., skipjack, yellowfin, bigeye, albacore and bluefin tunas. Typical tropical tuna species like skipjack and yellowfin are thought to spawn opportunistically in warm waters, and do not show clear spawning seasonality. With increasing affinities for colder waters and longer lifespan, in relation also with the extension of the feeding habitat to the temperate regions, other tuna species appear to develop such seasonality, lightly marked for bigeye, more evident for albacore and fully obvious for the temperate bluefin tuna (e.g., Fromentin and Powers, 2005). Also, with the increasing seasonal effect, the spawning grounds seem to become more limited in space (and time by definition), but likely more favorable to larval survival. This is a good illustration of an evolutionary contrast between *r*- and *K*- strategies. In a *r*-situation, organisms invest in quick reproduction, usually as an adaptation to a risky environment. This is clearly the case for skipjack, whose the main habitat, i.e., the western and central equatorial Pacific, is under the influence of the interannual (unpredictable) El Niño Southern Oscillation signal (Lehodey et al., 1997, 2003; Lehodey, 2001). In a *K*-situation, species invest in prolonged development and long life, in a more stable environment. Bluefin is a typical example, with clear seasonal (predictable) migrations between feeding grounds in rich temperate waters and spawning grounds in relatively limited favorable areas (e.g., Fromentin and Powers, 2005). The gradation in the ecology of these tuna species is another important feature that should help in the evaluation of the model because the coherent and consistent parameter values between these species should emerge from future optimization experiments.

On the other hand, since the model is driven by physical and biogeochemical oceanic variables, the accuracy of its predictions

strongly depend on the reliability of these variables. Here we used a coupled ocean-biogeochemical model primarily developed for investigating tropical regions (Murtugudde et al., 1996; Christian et al., 2002) and driven by atmospheric forcing (NCEP reanalysis). Though this model reproduces reasonably well the seasonal and interannual variability (Christian et al., 2002), it does display systematic biases in some regions, especially temperate ones, and was not configured here to resolve the mesoscale features that can play an important role in the dynamics of marine populations. In addition, at the time of these simulations, dissolved oxygen fields were available only as seasonal climatologies which is another potential source of biases for interannual variability. Therefore, we can expect that the parameter optimization techniques together with the rapid progress in the modeling of physical and biogeochemical oceanic environment, in particular with the increasing use of data assimilation, will considerably improve the prediction skills of future simulations. At the same time, it will be important to test multiple configurations of bio-physical outputs that can serve as forcing for the model and thus produce an envelope (or ensemble) of predictions, a more reliable result than any single simulation (Krishnamurti et al., 1999).

SEAPODYM combines bottom-up and top-down mechanisms, and intra- (i.e., between cohorts) and inter-species interactions. Natural mortality of a predator cohort can be locally affected by availability of forage, in relation to their own and all other predators' food requirement, but there is no feedback here on the mortality of forage groups, since it is pre-calculated (Lehodey, 2004) and thus controlled primarily by physical/environmental conditions. On the other hand, the spawning and recruitment processes depend on both food and predation density on larvae, as well as a relationship with spawning biomass. Our simulations have demonstrated that the food competition mechanism can produce very substantial changes in spatio-temporal distribution of natural mortality. These changes can modify drastically the conclusions of a fishery and ecosystem assessment study. Therefore, it will be of particular importance in the future to run parameter optimization experiments with multi-species configurations, as well as to test the sensitivity of optimization to the mid-trophic sub-model parameterization.

Any model is a simplified view of a system focusing on mechanisms that their authors consider essential. Thus, it is always worthwhile to compare simulations for the same system carried out with different classes of models. For tuna and pelagic ecosystem in the Pacific Ocean, such comparative analyses can include the statistical stock assessment models MULTIFAN-CL (Hampton and Fournier, 2001) and A-SCALA (Maunder and Watters, 2003), the ecotrophic model ECOPATH (Cox et al., 2002; Kitchell et al., 2002; Watters et al., 2003), or the ADR-bioenergetic model APECOSM (Maury et al., 2007). They should help in investigating bottom-up and top-down effects in the ecosystem. These studies will be part of the analyses planned through the international network of collaboration developed with the GLOBEC/CLIOTOP (CLimate Impacts on Oceanic TOp Predators) research program (Maury and Lehodey, 2005). The configuration of the model offers also an ideal tool to investigate the potential impacts of climate warming on tuna populations.

Acknowledgements

Appendix. Major notations

For simplicity, notations of species (sp), space (i, j) and time (t) are omitted.

z	Vertical layer, total number of layers is 3	
V_z	Vector (u, v) of horizontal currents	m s^{-1}
T_z	Temperature, available for each z	°C
O_z	Concentration of dissolved oxygen, available for each z	ml l^{-1}
P	Primary production, vertically integrated	g m^{-2} d^{-1}
F'_n	Production of immature forage (source for forage) density per unit of time step (six components)	g m^{-2}
F_n	Biomass (density) of mature forage populations (six components)	g m^{-2}
J_a	Density of juvenile age class of predator (tuna) population in number	
N_a	Density of adult age class a of predator (tuna) population in number	
B_a	Biomass of adult age class a of predator (tuna) population	g m^{-2}
R	New recruits to predator (tuna) population in number	
F_p	Biomass of forage potentially feeding on larvae	g m^{-2}
B_{adult}	Total biomass of immature and mature adult predators	g m^{-2}
l_a	Predator' size of cohort a	m
w_a	Predator'weight of cohort a	g
I_0	Larvae's habitat index (only one cohort in present configuration)	
$I_{1,k}$	Juvenile's habitat index of cohort k	
$I_{2,a}$	Adult's habitat index of cohort a	
H_S	Spawning habitat index	
$H_{F,a}$	Feeding habitat index of cohort a	
$\Theta_{a,n}$	Accessibility coefficient of predator (tuna) cohort a to forage component n	
$\vartheta_{n,a}$	Accessibility coefficient of predator cohort a to forage component n relative to all forage components	
d	Day-length function of latitude and date	h
G_d	Gradient of day-length	h d^{-1}
G_{max}	Maximum gradient of standardized habitat	
$G_x(G_y)$	Gradient of habitat index in the x (y)-direction	
$D_{a\,max}$	Maximum diffusion coefficient for cohort a (at size l_a)	nmi^2 month^{-1}
D_a	Diffusion coefficient for cohort a (at size l_a)	nmi^2 month^{-1}
χ	Taxis coefficient	nmi d^{-1}
$I_{FR,a}$	Food requirement index of cohort a	
F_{Rn}	Total requirement of forage component n	g
ω_n	Mortality of forage component n due to all predator cohorts	
M_P	Tuna predation mortality	time^{-1}
M_S	Tuna senescence mortality	time^{-1}

Parameters to be defined/estimated			unit	skipjack	bigeye
Population structure					
1		Number of larvae cohorts	Month	1	1
2		Number of juvenile cohorts	Month	2	2
3		Age at first autonomous displacement	Month	4	4
4		Number of young (immature) cohorts	Quarter	3	9
5		Age at first maturity	Quarter	4	10
6		Number of adult cohorts	Quarter	12	30
Growth					
7		Size-at-age	m	[a]	[a]
8		Weight-at-age	kg	[a]	[a]
Habitats					
9	T_s	Optimum of the spawning temperature function	°C	29	26
10	σ_s	Std. Err. of the spawning temperature function	°C	2	2
11	α	Larvae food–predator trade-off coefficient	–	1	3
12	T_a	Optimum of the adult temperature function at maximum age	°C	26	13
13	σ_a	Std. Err. of the adult temperature function at maximum age	°C	3	3
14	$\widehat{O}$	Oxygen value at $\Psi_O = 0.5$	ml l^{-1}	3	1
15	γ	Curvature coefficient of the oxygen function	–	−8	−8
16	κ	Curvature parameter in the function to switch continuously from feeding to spawning habitat	–	1000	1000
17	$\widehat{G}_d$	Threshold in the gradient of day-length at which the switch occurs between spawning and feeding habitat	h d^{-1}	0.015	0.025
Movements					
18	V_M	Maximum sustainable speed	Body Length s^{-1}	1	0.5
19	c	Coefficient of diffusion habitat dependence (defines the curvature and the minimum asymptotic value of the function)	–	0.1	0.1
20	η	Coefficient of diffusion density dependence (defines the curvature and the maximum asymptotic value of the function)	–	20	20
Food requirement					
21	r	Daily ration (relative to weight at age)	–	0.1	0.05
22	ρ	Coefficient of the Food requirement index function	–		0.02
Larvae recruitment					
23	R_s	Coefficient of larvae recruitment	–	0.2	0.001
Mortality					
24	$M_{P_{max}}$	Maximal mortality rate due to predation	Month^{-1}	0.3	0.083
25	$M_{S_{max}}$	Maximal mortality rate due to senescence	Month^{-1}	0.153	0.077
26	β_P	Slope coefficient in predation mortality	–	0.057	0.057
27	β_S	Slope coefficient in senescence mortality	–	−0.167	−0.167
28	$A_{0.5}$	Age at which $1/2\ M_{S_{max}}$ occurs	Month	30	36
29	ε	Coefficient of variability of tuna mortality with food requirement index	–	0.5	0.2

[a] From independent studies (Langley et al., 2005; Hampton et al., 2006).

References

Bertignac, M., Lehodey, P., Hampton, J., 1998. A spatial population dynamics simulation model of tropical tunas using a habitat index based on environmental parameters. Fisheries Oceanography 7, 326–334.

Bertrand, A., Bard, F.X., Josse, E., 2002. Tuna food habits related to the micronekton distribution in French Polynesia. Marine Biology 140, 1023–1037.

Block, B.A., Teo, S.L.H., Walli, A., Stokesbury, M.J.W., Farwell, C.J., Weng, K.C., Dewar, H., Williams, T.D., 2005. Electronic tagging and population structure of Atlantic bluefin tuna. Nature 234, 1121–1127.

Brill, R.W., 1994. A review of temperature and oxygen tolerance studies of tunas pertinent to fisheries oceanography, movement models and stock assessments. Fisheries Oceanography 3, 204–216.

Brill, R.W., Bigelow, K.A., Musyl, M.K., Fritsches, K.A., Warrant, E.J., 2005. Bigeye tuna (*Thunnus obesus*) behavior and physiology and their relevance to stock assessments and fishery biology. ICCAT, Collective Volume of Scientific Papers, 57(2), 142–161.

Christian, J., Verschell, M., Murtugudde, R., Busalacchi, A., McClain, C., 2002. Biogeochemical modeling of the tropical Pacific Ocean I: seasonal and interannual variability. Deep Sea Research II 49, 509–543.

Cox, S.P., Essington, T.E., Kitchell, J.F., Martell, S.J.D., Walters, C.J., Boggs, C., Kaplan, I., 2002. Reconstructing ecosystem dynamics in the central Pacific Ocean, 1952–1998. II. A preliminary assessment of the trophic impacts of fishing and effects on tuna dynamics. Canadian Journal of Fisheries and Aquatic Sciences 59 (11), 1736–1747.

Cury, P., 1994. Obstinate nature: an ecology of individuals: thoughts on reproductive biology and biodiversity. Canadian Journal of Fisheries and Aquatic Sciences 51, 1664–1673.

Cushing, D.H., 1975. Marine Ecology and Fisheries. Cambridge University Press, Cambridge, England. p. 278.

Fromentin, J.-M., Powers, J.E., 2005. Atlantic bluefin tuna: population dynamics, ecology, fisheries and management. Fish and Fisheries 6, 281–306.

Hampton, J., Fournier, D., 2001. A spatially disaggregated, length-based, age-structured population model of yellowfin tuna (*Thunnus albacares*) in the western and central Pacific Ocean. Marine Freshwater Research 52, 937–963.

Hampton, J., Bigelow, K.A., Labelle, M., 1998. A summary of current information on the biology, fisheries and stock assessment of bigeye tuna (*Thunnus obesus*) in the Pacific Ocean, with recommendations for data requirements and future research. Noumea, New Caledonia, Secretariat of the Pacific Community. Technical Report 36, 1–46.

Hampton, J., Langley, A., Kleiber, P., 2006. Stock assessment of bigeye tuna in the western and central Pacific Ocean, including an analysis of management options. In: 2nd Meeting of the Scientific Committee of the Western and Central Pacific Fisheries Commission, Manila, Philippines, 7–18 August 2006. WCPFC-SC2-SA WP-2, 103 pp.

Holland, K.N., Brill, R.W., Chang, R.K., Sibert, J.R., Fournier, D.A., 1992. Physiological and behavioral thermoregulation in bigeye tuna (*Thunnus obesus*). Nature 358, 110–112.

King, J.E., Ikehara, I.I., 1956. Comparative study of the food of the bigeye and yellowfin tuna in the central Pacific. US National Marine Fisheries Service. Fishery Bulletin 57, 61–85.

Kitchell, J.F., Essington, T.E., Boggs, C.H., Schindler, D.E., Walters, C.J., 2002. The role of sharks and longline fisheries in a pelagic ecosystem of the Central Pacific. Ecosystems 5, 202–216.

Krishnamurti, T.N., Kishtawal, C.M., LaRow, T.E., Bachiochi, D.R., Zhang, Z., Williford, C.E., Gadgil, S., Surendran, S., 1999. Improved weather and seasonal climate forecasts from multimodel superensemble. Science 285, 1548–1550.

Langley, A., Hampton, J., Ogura, M., 2005. Stock assessment of skipjack tuna in the western and central Pacific Ocean. In: 1st Meeting of the Scientific Committee of the Western and Central Pacific Fisheries Commission, Noumea, New Caledonia, 8–19 August 2005, WCPFC-SC1 SA WP-4, 69 pp.

Lehodey, P., 2001. The pelagic ecosystem of the tropical Pacific Ocean: dynamic spatial modeling and biological consequences of ENSO. Progress in Oceanography 49, 439–468.

Lehodey, P., 2004. A Spatial Ecosystem And Populations Dynamics Model (SEAPODYM) for tuna and associated oceanic top-predator species: Part I – lower and intermediate trophic components. In: 17th Meeting of the Standing Committee on Tuna and Billfish, Majuro, Republic of Marshall Islands, 9–18 August 2004. Oceanic Fisheries Programme, Secretariat of the Pacific Community, Noumea, New Caledonia, SCTB Working Paper ECO-1, 26 pp. <http://www.spc.int/oceanfish/Html/SCTB/SCTB17/ECO-1.pdf>.

Lehodey, P., Bertignac, M., Hampton, J., Lewis, T., Picaut, J., 1997. El Niño Southern Oscillation and Tuna in the western Pacific. Nature 389, 715–718.

Lehodey, P., André, J.-M., Bertignac, M., Hampton, J., Stoens, A., Menkès, C., Memery, L., Grima, N., 1998. Predicting skipjack tuna forage distributions in the Equatorial Pacific using a coupled dynamical bio-geochemical model. Fisheries Oceanography 7, 317–325.

Lehodey, P., Chai, F., Hampton, J., 2003. Modeling climate-related variability of tuna populations from a coupled ocean-biogeochemical-populations dynamics model. Fisheries Oceanography 12 (4), 483–494.

Maunder, M.N., Watters, G.M., 2003. A-SCALA: an age-structured statistical catch-at-length analysis for assessing tuna stocks in the Eastern Pacific Ocean. Inter-American Tropical Tuna Commission Bulletin 22 (5), 433–582.

Maury, O., 2005. How to model the size-dependent vertical behavior of bigeye (*Thunnus obesus*) tuna in its environment? Col. Vol. Sci. Pap. ICCAT 57 (2), 115–126.

Maury, O., Lehodey, P. (Eds.), 2005. Climate Impacts on Oceanic TOp Predators (CLIOTOP). Science Plan and Implementation Strategy. GLOBEC Report No. 18, ii, 42pp.

Maury, O., Faugeras, B., Shina, Y.-J., Poggialeb, J.-C., Ben Aria, T., Marsac, F., 2007. Modeling environmental effects on the size-structured energy flow through marine ecosystems. Part 1: the model. Progress in Oceanography 74, 479–499.

Megrey, B.A., Rose, K.A., Klumb, R.A., Hay, D.E., Werner, F.E., Eslinger, D.L., Smith, S.L., 2007. A bioenergetics-based population dynamics model of Pacific herring (*Clupea harengus pallasii*) coupled to a lower trophic level nutrient–phytoplankton–zooplankton model: description, calibration and sensitivity analysis. Ecological Modelling 202, 144–164.

Murtugudde, R., Seager, R., Busalacchi, A., 1996. Simulation of the tropical oceans with an ocean GCM coupled to an atmospheric mixed layer model. Journal of Climate 9, 1795–1815.

Nishikawa, Y., Honma, M., Ueyenagi, S., Kikawa, S., 1985. Average distribution of larvae of oceanic species of scombrid fishes, 1951–81. Contribution of the Far Seas Fisheries Research Laboratory, Fishery Agency of Japan, 236, 1–99.

Okamura, H., 2008. Brain comes to light. Nature 452, 294–295.

Okubo, A., 1980. Diffusion and ecological problems: mathematical models. Springer-Verlag, NY.

Schaefer, K.M., Fuller, D.W., 2002. Movements, behavior, and habitat selection of bigeye tuna (*Thunnus obesus*) in the eastern equatorial Pacific, ascertained through archival tags. Fishery Bulletin 100, 765–788.

Senina, I., Sibert, J., Lehodey, P., 2008. Parameter estimation for basin-scale ecosystem-linked population models of large pelagic predators: application to skipjack tuna. Progress in Oceanography 78 (4), 319–335.

Sharp, G.D., 1978. Behavioral and physiological properties of tuna and their effects on vulnerability to fishing gear. In: Sharp, G.D., Dizon, A.E. (Eds.), The Physiological Ecology of Tunas. Academic Press, New York, pp. 397–449.

Sibert, J.R., Hampton, J., Fournier, D.A., Bills, P.J., 1999. An advection–diffusion-reaction model for the estimation of fish movement parameters from tagging data, with application to skipjack tuna (*Katsuwonus pelamis*). Canadian Journal of Fisheries and Aquatic Sciences 56, 925–938.

Sund, P.N., Blackburn, M., Williams, F., 1980. Tunas and their environment in the Pacific Ocean: a review. Oceanography Marine Biology Annual Review 19, 443–512.

Wang, X., Christian, J.R., Murtugudde, R., Busalacchi, A.J., 2005. Ecosystem dynamics and export production in the central and eastern equatorial Pacific: a modeling study of impact of ENSO. Geophysical Research Letter 32, L2608.

Watters, G.M., Olson, R.J., Francis, R.C., Fiedler, P.C., Polovina, J.J., Reilly, S.B., Aydin, K.Y., Boggs, C.H., Essington, T.E., Walters, C.J., Kitchell, J.F., 2003. Physical forcing and the dynamics of the pelagic ecosystem in the eastern tropical Pacific: simulations with ENSO-scale and global-warming climate drivers. Canadian Journal of Fisheries and Aquatic Sciences 60, 1161–1175.